



CORPUS PUBLISHERS

# Journal of Mineral and Material Science (JMMS)

ISSN: 2833-3616

Volume 7 Issue 2, 2026

## Article Information

Received date : March 14, 2026

Published date: April 06, 2026

## \*Corresponding author

Abdulelah Mari Alqarni, Department of Mechanical Engineering, Faculty of Engineering, King Abdulaziz University, Jeddah and Riyadh Region Municipality, Saudi Arabia

DOI: 10.54026/JMMS/1135

## Key Words

MAX Phases; Magnesium Alloys; Friction Stir Processing; Thermal Conductivity; Electrical Conductivity; Coefficient of Thermal Expansion

Distributed under Creative Commons CC-BY 4.0

Research Article

# Influence of MAX-Phase Reinforcements on the Electrical and Thermal Behavior of AZ<sup>31</sup> Magnesium Matrix Composites Fabricated Via Friction Stir Processing

Alqarni AM<sup>1,2\*</sup>, Bamasag A<sup>2</sup> and Ahmed I<sup>2</sup><sup>1</sup>Riyadh Region Municipality, Saudi Arabia<sup>2</sup>Department of Mechanical Engineering, Faculty of Engineering, King Abdulaziz University, Jeddah, Saudi Arabia

## Abstract

Magnesium alloys are being used more and more in lightweight structural applications, but their high thermal expansion and low thermal stability make them hard to use widely. This study examines the electrical and thermal characteristics of AZ31 magnesium alloy matrix composites augmented with MAX-phase particles (Ti<sub>3</sub>AlC<sub>2</sub>, V<sub>2</sub>AlC, and Cr<sub>2</sub>AlC) produced through Friction Stir Processing (FSP). The findings indicate that the integration of MAX-phase improves dimensional stability, albeit at the expense of transport properties. The electrical conductivity dropped from 21.8 MS/m for monolithic AZ31 to between 19.42 and 20.12 MS/m for the composites. This was because electrons scattered at the interfaces between the matrix and the reinforcement and because of defects caused by FSP. Thermal conductivity showed a small drop, going from 139.29 to 146.22 W/m·K, because of phonon scattering (Kapitza resistance). On the other hand, the coefficient of thermal expansion (CTE) dropped by 23-25%, from  $23.2 \times 10^{-6}/^{\circ}\text{C}$  for AZ31 to  $17.4\text{-}17.8 \times 10^{-6}/^{\circ}\text{C}$  for the composites. V<sub>2</sub>AlC had the most balanced profile of the reinforcements, keeping the highest thermal conductivity, while Cr<sub>2</sub>AlC had better dimensional stability. These results show that MAX-phase reinforced Mg-MMCs could be useful for thermal management tasks that need very precise dimensional control.

## Introduction

Magnesium (Mg) and its alloys, especially AZ31, are known to be the lightest structural metals that can be used in engineering. They have a density of about 1.74 g/cm<sup>3</sup> [1]. Due to their high specific strength and ability to dampen vibrations, they are great for the automotive, aerospace, and portable electronics industries [2]. However, their use in high-performance environments is limited by their high Coefficients of Thermal Expansion (CTE), low wear resistance, and low thermal stability at high temperatures [3]. To address these limitations, Metal Matrix Composites (MMCs) fortified with ceramic particles have been created. Traditional reinforcements such as SiC and Al<sub>2</sub>O<sub>3</sub> frequently exhibit inadequate interfacial compatibility and significant CTE mismatches, resulting in residual stresses [4]. MAX phases (M<sub>n+1</sub>AX<sub>n</sub>), a group of layered ternary carbides and nitrides, have become promising reinforcements because they have a unique mix of metallic and ceramic properties, such as high thermal stability, damage resistance, and adjustable electrical conductivity [5]. Friction Stir Processing (FSP) provides a solid-state method for integrating these reinforcements, avoiding the porosity and interfacial degradation typical in liquid-phase processing [6]. MAX phases strengthen Matrices Made of Metal (MRM) and Polymer (MRP).

Gupta et al. [7] say that they have different stages of friction and wear at room temperature. These nanolaminates have both metal and ceramic properties, which makes them stronger, stiffer, and better at conducting heat [8]. They can be used in electronics, aerospace, and sensing technologies because they can handle heat well, resist corrosion, and have adjustable electrical properties [9]. Recent progress in nanostructured MAX phases has sparked interest in research for high-temperature and nuclear applications [10]. Adding Ti<sub>3</sub>SiC<sub>2</sub> makes polymers harder and stronger by delaying third-body abrasion. MAX phases, on the other hand, don't wear down or create friction at high temperatures [11]. Prior research has predominantly concentrated on mechanical improvements; however, there exists a deficiency of systematic studies correlating MAX-phase chemistry with the functional electrical and thermal characteristics of Mg-based composites. This study seeks to address this deficiency by assessing the electrical conductivity, thermal conductivity, and thermal expansion characteristics of AZ31 composites augmented with Ti<sub>3</sub>AlC<sub>2</sub>, V<sub>2</sub>AlC, and Cr<sub>2</sub>AlC MAX phases. The electrical and thermal properties of MAX phases are essential factors influencing their efficacy in functional applications, demonstrating considerable variability contingent upon chemical composition and stoichiometry. Ti<sub>3</sub>AlC<sub>2</sub> and Cr<sub>2</sub>AlC are better at conducting electricity than other materials. Their conductivity is about  $3.48 \times 10^6 \Omega^{-1}\text{m}^{-1}$  and  $3.45 \times 10^6 \Omega^{-1}\text{m}^{-1}$ , respectively, which means they have low resistivity values of  $0.29 \times 10^{-6} \Omega\text{-m}$  [12]. On the other hand, Ti<sub>4</sub>AlN<sub>3</sub> has much lower conductivity ( $0.5 \times 10^6 \Omega^{-1}\text{m}^{-1}$ ) and higher resistivity ( $2 \times 10^{-6} \Omega\text{-m}$ ). This is because the charge carriers don't move around as easily. Ta<sub>4</sub>AlC<sub>3</sub>, Ti<sub>2</sub>AlC, and Nb<sub>4</sub>AlC<sub>3</sub> have intermediate values, with conductivities between  $1.33$  and  $2.59 \times 10^6 \Omega^{-1}\text{m}^{-1}$  [13-15]. All phases act like metals, with positive temperature resistivity coefficients that range from  $0.002 \text{ K}^{-1}$  for Ti<sub>2</sub>AlC to  $0.0075 \text{ K}^{-1}$  for Ti<sub>4</sub>AlN<sub>3</sub>. This means that electronic resistance goes up in a straight line as temperature goes up. Thermal properties further set these materials apart, especially when it comes to how they move heat and expand. Ta<sub>4</sub>AlC<sub>3</sub> has the highest thermal conductivity at room temperature, at  $38.4 \text{ W}\cdot\text{m}^{-1}\text{K}^{-1}$ . This is much higher than Nb<sub>4</sub>AlC<sub>3</sub> ( $13.5 \text{ W}\cdot\text{m}^{-1}\text{K}^{-1}$ ), Cr<sub>2</sub>AlC ( $17.9 \text{ W}\cdot\text{m}^{-1}\text{K}^{-1}$ ), and Ti<sub>4</sub>AlN<sub>3</sub> ( $12 \text{ W}\cdot\text{m}^{-1}\text{K}^{-1}$ ) [16]. Most phases have thermal expansion coefficients between  $7.2 \times 10^{-6} \text{ K}^{-1}$  (Nb<sub>4</sub>AlC<sub>3</sub>) and  $9.7 \times 10^{-6} \text{ K}^{-1}$  (Ti<sub>4</sub>AlN<sub>3</sub>).

However, Cr<sub>2</sub>AlC is an exception because it has a much higher value of  $13.3 \times 10^{-6} \text{ K}^{-1}$ . The heat capacity values are different, with Ta<sub>4</sub>AlC<sub>3</sub> having the highest value (185 J·mol<sup>-1</sup>·K<sup>-1</sup>) and Ti<sub>2</sub>AlC and Cr<sub>2</sub>AlC having lower values (around 84-87 J·mol<sup>-1</sup>·K<sup>-1</sup>). These variations highlight the tunability of MAX phases, allowing for the selection of specific combinations of M, A, and X elements to customize electrical and thermal responses for specific engineering needs. This study seeks to address the existing gap by methodically assessing the impact of MAX-phase chemistry on the functional electrical and thermal properties of AZ31 magnesium alloy matrix composites produced through Friction Stir Processing. The study examines the electrical conductivity, thermal conductivity, and coefficient of thermal expansion of AZ31 composites enhanced with Ti<sub>3</sub>AlC<sub>2</sub>, V<sub>2</sub>AlC, and Cr<sub>2</sub>AlC particles. This study aims to facilitate application-specific reinforcement selection for next-generation lightweight composites in thermal management and high-performance structural contexts by correlating reinforcement type with transport properties and dimensional stability.

## Materials and Methods

### Materials

The matrix material was made up of rolled sheets of AZ31 magnesium alloy that were  $150 \times 150 \times 10 \text{ mm}^3$  in size. There was 2.5-3.5 wt% Al, 0.6-1.4 wt% Zn, and the rest was Mg in the chemical makeup. The reinforcement powders were Ti<sub>3</sub>AlC<sub>2</sub>, V<sub>2</sub>AlC, and Cr<sub>2</sub>AlC MAX phases with particle sizes of 1 to 5 μm and purities of more than 98.5%.

### Composite fabrication

Composites were fabricated using Friction Stir Processing (FSP) on a vertical CNC milling machine. The AZ31 plates were machined with a groove to hold the reinforcement powder. We used a hardened H13 steel tool with a triangular pin profile (8 mm diameter, 6 mm length) and a shoulder diameter of 25 mm [17]. The processing parameters were kept at a rotation speed of 800 rpm, a traverse speed of 30 mm/min, and a tilt angle of 3° [18]. Before the composite was processed with friction stir, the sheets were prepared by making a regular pattern of holes that were 3 mm wide and 2 mm deep to hold the reinforcement mixture.

### Characterization

- Electrical Conductivity: Measured with a Keithley 6517B Electrometer using the four-point probe method to get rid of contact resistance. The measurements were done at 30°C [19].
- Thermal Conductivity: Measured at room temperature (25°C) with a Hongjin Thermal Conductivity Tester (model HJ-TC) that uses Transient Plane Source (TPS) technology.
- Thermal Expansion: A Netzsch DIL 402 PC dilatometer measured the coefficient of thermal expansion (CTE) from 30°C to 500°C at a rate of 5°C/min in an argon atmosphere.
- Microstructure: We used Scanning Electron Microscopy (SEM) and energy-dispersive X-ray spectroscopy (EDS) to check the distribution of particles and the integrity of the interface.

## Results and Discussion

### Physical properties

The Metal Matrix Composites (MMCs) were fabricated via a modified Friction Stir Processing (FSP) route. Rolled Magnesium AZ31 alloy sheets ( $150 \times 150 \times 10 \text{ mm}^3$ ) served as the matrix material. To introduce the reinforcement phase, a central longitudinal groove was machined into each plate using CNC milling, with dimensions strictly controlled at width  $w = 3 \text{ mm}$ , depth  $d = 2 \text{ mm}$ , and length  $l = 100 \text{ mm}$ . Three distinct MAX-phase powders—Ti<sub>3</sub>AlC<sub>2</sub>, V<sub>2</sub>AlC and Cr<sub>2</sub>AlC—were individually packed into the grooves of separate plates to produce three composite systems:  $\frac{\text{AZ31}}{\text{Ti}_3\text{AlC}_2}$ , AZ31/V<sub>2</sub>AlC, and AZ31/Cr<sub>2</sub>AlC.

**Volume fraction and weight percentage calculations:** The theoretical reinforcement volume fraction ( $V_f$ ) was determined by the ratio of the packed powder volume ( $V_p$ ) to the effective stir zone volume ( $V_{sz}$ ) defined by the tool pin geometry (diameter  $D = 8 \text{ mm}$ , length  $L = 6 \text{ mm}$ ). The reinforcement volume was calculated as:  $V_p = w \cdot d \cdot l = 3.2 \cdot 100 = 320 \text{ mm}^3$ . The stir zone volume swept by the rotating pin is given by:

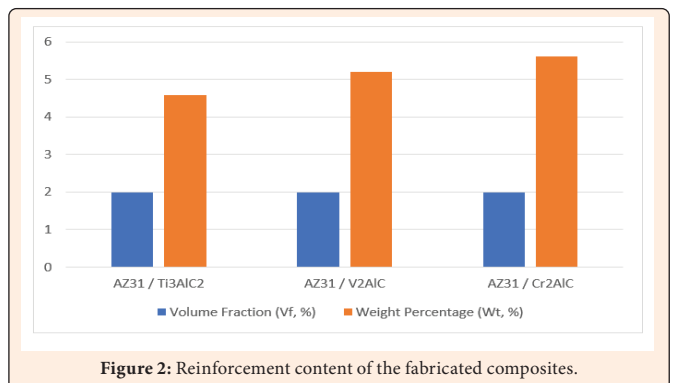
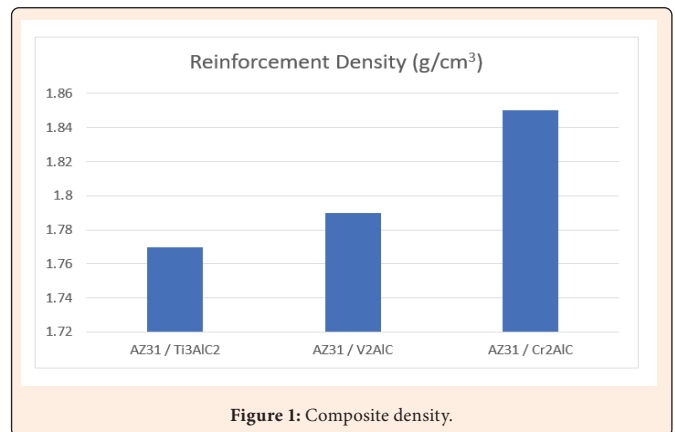
$$V_{sz} = \frac{\pi \cdot D^2}{4} \cdot L \cdot l \approx 30.159 \text{ mm}^3$$

Accordingly, the calculated volume fraction for all composite variants was  $V_f \approx 2\%$ . Corresponding weight percentages ( $W_f$ ) were derived using the rule of mixtures, incorporating the specific densities of each MAX-phase ( $\rho_p$ ) the AZ31 matrix ( $\rho_m \approx 1.77 \frac{\text{g}}{\text{cm}^3}$ ), as summarized in Table 1.

The compositional analysis of the three AZ31-based MAX-phase composite systems shows that all of them had a consistent theoretical volume fraction of 2% (Figures 1 & 2). However, the weight percentages varied a lot because the densities of the reinforcements were different. The reinforcement density chart (Figure 3) shows that the MAX-phase particles' density increased from Ti<sub>3</sub>AlC<sub>2</sub> (4.2 g/cm<sup>3</sup>) to V<sub>2</sub>AlC (4.8 g/cm<sup>3</sup>) to Cr<sub>2</sub>AlC (5.2 g/cm<sup>3</sup>). This directly affected the weight percentage calculations in Figure 1. So, even though the volumetric reinforcement content was the same, the weight percentages went up from 4.58 wt% for AZ31/Ti<sub>3</sub>AlC<sub>2</sub> to 5.20 wt% for AZ31/V<sub>2</sub>AlC and finally to 5.61 wt% for AZ31/Cr<sub>2</sub>AlC. This increase in weight percentage of about 22.5% from the Ti-based to the Cr-based composite, even though the volume fractions are the same, is because chromium has a higher atomic mass than titanium and vanadium in the MAX-phase crystal structures. The constant volume fraction across all systems guarantees that subsequent variations in mechanical, thermal, and electrical properties can be ascribed to the inherent characteristics of each MAX-phase reinforcement, rather than disparities in reinforcement content. This facilitates a systematic assessment of the impact of transition metal chemistry on composite performance.

**Table 1:** Physical properties and reinforcement content of the fabricated composites.

Composite System	Reinforcement Density (g/cm <sup>3</sup> )	Volume Fraction (V <sub>p</sub> %)	Weight Percentage (W <sub>p</sub> %)
AZ31/Ti <sub>3</sub> AlC <sub>2</sub>	4.2	2	4.58
AZ31/V <sub>2</sub> AlC	4.8	2	5.2
AZ31/Cr <sub>2</sub> AlC	5.2	2	5.61



### Microstructural evolution and particle distribution

Figure 3 shows SEM micrographs that show the surface morphology and reinforcement distribution in the composites that were made. The monolithic AZ31 alloy (Figure 3a) shows a microstructure that is fairly uniform, with grain boundaries that are typical of FSP-processed material. The reinforced composites (Figure 3b-3d), on the other hand, clearly show bright MAX-phase particles spread out over the darker magnesium matrix. The  $V_2AlC$ -reinforced composite (Figure 1) has separate reinforcement particles that don't group together very much. On the other hand, the  $Ti_3AlC_2$  composite (Figure 3c) has a higher density of particles spread out across the stir zone. The  $Cr_2AlC$ -reinforced composite (Figure 3d) also has well-dispersed particles, but there are some areas where particles are grouped together. The overall particle distribution seen in these micrographs supports the idea that the FSP method works well to break up initial powder agglomerates and achieve a fairly uniform reinforcement dispersion within the AZ31 matrix. This is important for improving the mechanical and functional properties of the resulting surface composites. The SEM-EDS test showed that all three MAX-phase reinforcements were successfully added to the AZ31 matrix. The FSP process effectively broke up particle agglomerates and spread them out evenly across the stir zone, which is what you would expect from solid-state processing, which involves severe plastic deformation and dynamic recrystallization. Elemental mapping confirmed the presence of characteristic signatures: Ti (6.23 wt%) for  $Ti_3AlC_2$ , V (57.83 wt%) for  $V_2AlC$ , and Cr (37.98 wt%) for  $Cr_2AlC$  composites. The high aluminum content in all of the composites, which was higher than the base AZ31 composition (~3 wt%), showed that both the matrix and the reinforcement phases were working together. There were very few voids or debonding in the interfacial regions, which shows that FSP's intense stirring action made the mechanical bond work well.

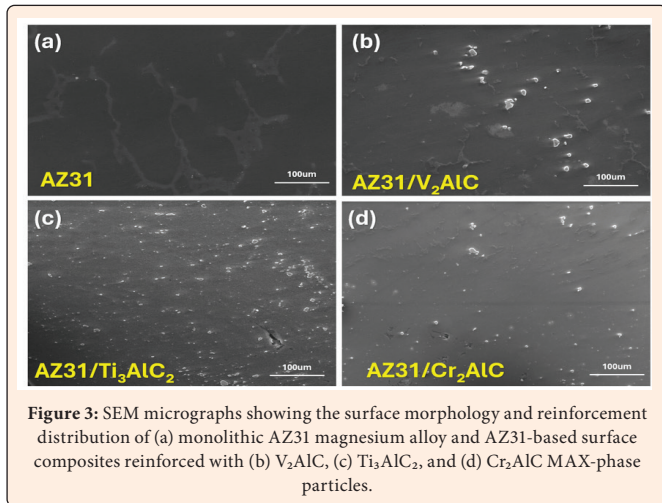


**Figure 3:** SEM micrographs showing the surface morphology and reinforcement distribution of (a) monolithic AZ31 magnesium alloy and AZ31-based surface composites reinforced with (b)  $V_2AlC$ , (c)  $Ti_3AlC_2$ , and (d)  $Cr_2AlC$  MAX-phase particles.

### Electrical conductivity

Adding MAX-phase reinforcements made the electrical conductivity lower than that of the monolithic AZ31 alloy. Figure 4 shows that AZ31's baseline conductivity was 21.8 MS/m. The composites had these values: AZ31/ $Ti_3AlC_2$  (20.12 MS/m), AZ31/ $Cr_2AlC$  (19.84 MS/m), and AZ31/ $V_2AlC$  (19.42 MS/m).

This decrease is due to a number of factors that are all connected. First, reinforcement scattering happens when MAX phases, which are conductive for ceramics, have lower conductivity than the Mg matrix. This makes it harder for electrons to flow. Second, the high level of plastic deformation that comes with FSP increases the density of dislocations, which creates more scattering centers [20]. Third, dynamic recrystallization-induced grain refinement makes grain boundary scattering stronger. Lastly, the interfacial resistance between the matrix and MAX phases changes with chemistry. The  $V_2AlC$  composite had the biggest drop, which suggests that certain electronic structure interactions at the  $V_2AlC/AZ31$  interface may make it harder for charges to move than Ti or Cr-based composites.

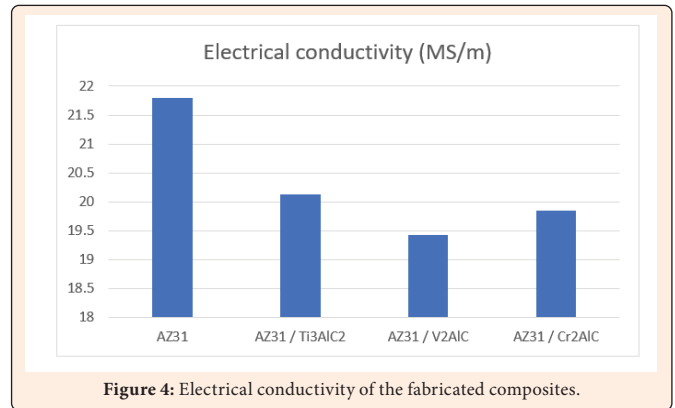


**Figure 4:** Electrical conductivity of the fabricated composites.

### Thermal conductivity

Thermal conductivity is important for getting rid of heat in structural parts. The monolithic AZ31 had a thermal conductivity of 150.22 W/m-K. Reinforcement caused drops of 2.66% to 7.28% (Figure 5). The order of thermal performance was: AZ31/ $V_2AlC$  (146.22 W/m-K) > AZ31/ $Cr_2AlC$  (142.79 W/m-K) > AZ31/ $Ti_3AlC_2$  (139.29 W/m-K). Interfacial thermal resistance, which is also called Kapitza resistance, is the main reason for this degradation. Phonons, the main carriers of heat, run into the interfaces between the AZ31 matrix and the MAX-phase particles, which act as scattering centers. The size of this resistance is determined by how well the two materials bond and how well they match in terms of sound. The  $V_2AlC$  composite exhibited superior retention of thermal conductivity, owing to the enhanced electron and phonon transport properties characteristic of vanadium-based MAX phases in comparison to titanium and chromium counterparts. Even though the values went down, all of the composites still had values higher than 139 W/m-K, which means they could still be used for thermal management.

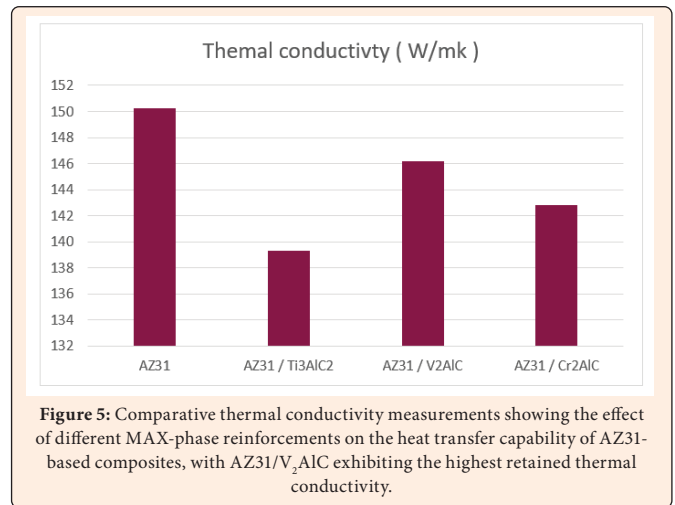


**Figure 5:** Comparative thermal conductivity measurements showing the effect of different MAX-phase reinforcements on the heat transfer capability of AZ31-based composites, with AZ31/ $V_2AlC$  exhibiting the highest retained thermal conductivity.

### Property trade-offs and selection

The data reveals a critical engineering trade-off. While mechanical properties (hardness and modulus) generally improved with reinforcement addition (as detailed in companion mechanical studies), thermal and electrical conductivities exhibited modest reductions.



- a)  $V_2AlC$  emerges as the most balanced option, delivering substantial mechanical enhancement while minimizing degradation of thermal conductivity (highest retention among reinforced systems).
- b)  $Cr_2AlC$  offers maximum stiffness and thermal expansion control but incurs the greatest thermal transport penalty.
- c)  $Ti_3AlC_2$  provides moderate mechanical gains with superior oxidation resistance at elevated temperatures but the lowest thermal conductivity retention [21].

## Conclusion

This study successfully demonstrated the viability of MAX-phase particles ( $Ti_3AlC_2$ ,  $V_2AlC$ , and  $Cr_2AlC$ ) as advanced reinforcements for AZ31 magnesium alloy matrix composites fabricated via Friction Stir Processing. The key conclusions are:

- a) Electrical Conductivity decreased by 7.7-10.9% relative to baseline AZ31, governed by electron scattering at interfaces and increased defect density from FSP-induced deformation.
- b) A modest reduction of 2.66-7.28% was observed, primarily due to interfacial phonon scattering (Kapitza resistance).  $V_2AlC$  reinforcements retained the highest thermal conductivity (146.22 W/m·K).
- c)  $V_2AlC$  is recommended for applications requiring efficient heat dissipation coupled with moderate dimensional stability (e.g., heat sinks), while  $Cr_2AlC$  is preferred for components subjected to severe thermal cycling where dimensional tolerance is paramount.

These findings enable application-specific reinforcement selection based on performance priorities, facilitating the design of next-generation lightweight composites for high-temperature structural and thermal management applications.

## References

1. Mordike BL, Ebert T (2001) Magnesium: properties - applications - potential. *Materials Science and Engineering: A* 302(1): 37-45.
2. Lattanzi L, Jarfors AEW (2025) Advances in metal matrix composites: structure, properties and applications. *Crystals* 15(12): 1016.
3. Edgar R, Schmid-Fetzer R, Grobner J, Kevorkov DG (2006) Magnesium alloys and their applications.
4. Wei B, Cao H, Song S (2010) RETRACTED: Environmental resistance and mechanical performance of basalt and glass fibers. *Materials Science and Engineering: A* 527(18-19): 4708-4715.
5. Barsoum MW (2000) The MN+1AXN phases: A new class of solids: thermodynamically stable nanolaminates. *Progress in Solid State Chemistry* 28(1): 201-281.
6. Sun N, Apelian D (2011) Friction stir processing of aluminum cast alloys for high performance applications. *JOM* 63(11): 44-50.
7. Gupta S, Hammann T, Johnson R, Riyad MF (2015) Tribological behavior of novel  $Ti_3SiC_2$  (natural nanolaminates)-reinforced epoxy composites during dry sliding. *Tribology Transactions* 58(3): 560-566.
8. Shao H, Luo S, Descamps-Mandine A, Ge K, Lin Z et al. (2023) Synthesis of MAX phase nanofibers and nanoflakes and the resulting MXenes. *Advanced Science* 10(1): 2205509.
9. Wang ZI, Zheng K, Xiong JY, Xun LJ, Han Y, et al. (2022) Ceramic precursor-phthalonitrile hybrid with improved high heat resistance through constructing binary continuous phases. *Composites Part A: Applied Science and Manufacturing* 162: 107123.
10. Li Y, Shao H, Lin Z, Lu J, Liu L, et al. (2020) A general Lewis acidic etching route for preparing MXenes with enhanced electrochemical performance in non-aqueous electrolyte. *Nat Mater* 19(8): 894-899.
11. Magnus C (2023) Sliding wear of MAX phase composites  $Ti_3SiC_2$ -TiC and  $Ti_3AlC_2$ - $Ti_2AlC$  at 400°C and the influence of counterface material (steel,  $Al_2O_3$ , and  $Si_3N_4$ ) on wear behaviour. *Wear* 516-517: 204588.
12. Bao YW, Wang X, Zhang HB, Zhou YC (2005) Thermal shock behavior of  $Ti_3AlC_2$  from between 200°C and 1300°C. *Journal of the European Ceramic Society* 25(14): 3367-3374.
13. Hu C, Li F, He L, Liu M, Zhang J, et al. (2008) In situ reaction synthesis, electrical and thermal, and mechanical properties of  $Nb_4AlC_3$ . *Journal of the American Ceramic Society* 91(7): 2258-2263.
14. Hu C, Lin Z, He L, Bao Y, Wang J, et al. (2007) Physical and mechanical properties of bulk  $Ta_4AlC_3$  ceramic prepared by an in situ reaction synthesis/hot-pressing method. *Journal of the American Ceramic Society* 90(8): 2542-2548.
15. Bai Y, He X, Zhu C, Chen G (2012) Microstructures, electrical, thermal, and mechanical properties of bulk  $Ti_2AlC$  synthesized by self-propagating high-temperature combustion synthesis with pseudo hot isostatic pressing. *Journal of the American Ceramic Society* 95(1): 358-364.
16. Qureshi MW, Ma X, Tang G, Miao B, Niu J (2021) Fabrication and mechanical properties of  $Cr_2AlC$  MAX phase coatings on  $TiBw/Ti_6Al_4V$  composite prepared by HiPIMS. *Materials* 14(4): 826.
17. Gazo-Hanna E, Moustafa EB, Mosleh AO, Amine S, Younes K (2025) Evaluating the influence of friction stir processing on  $AlSi7Mg0.2$  alloy using principal component analysis. *Results in Engineering* 27: 106021.
18. Almutairi SS, Mosleh AO, Mohamed SS, Mahmoud TS, Moustafa EB (2024) Max-phase  $Ti_3SiC_2$  and diverse nanoparticle reinforcements for enhancement of the mechanical, dynamic, and microstructural properties of AA5083 aluminum alloy via FSP. 13(1).
19. Essam B, Moustafa MAT (2020) Preparation of high strength graphene reinforced Cu-based nanocomposites via mechanical alloying method: microstructural, mechanical and electrical properties. *Applied Physics A* 126: 220.
20. Akbarpour MR, Mirabad HM, Gazani F, Khezri I, Chadegani AA, et al. (2023) An overview of friction stir processing of cu-sic composites: Microstructural, mechanical, tribological, and electrical properties. *Journal of Materials Research and Technology* 27: 1317-1349.
21. Dmitruk A, Naplocha K, Zak A, Strojny-Nędzka A, Dieringa H, et al. (2019) Development of pore-free Ti-Si-C MAX/Al-Si composite materials manufactured by squeeze casting infiltration. *Journal of Materials Engineering and Performance* 28(10): 6248-6257.